Dependency of nonuniform ground surface liquefaction damage on organization and slope of deep strata

Non-uniformité des dommages de liquéfaction de la couche de surface due à la configuration des strates profondes et de l'inclinaison des strates

Asaoka A.
Association for the Development of Earthquake Prediction, Japan
Nakai K.
Nagoya University, Japan

ABSTRACT: Urayasu City, Japan, experienced heavy liquefaction damage due to the Great East Japan Earthquake, and the damage was characteristically nonuniform and varied widely depending on the location. Variation in the level of liquefaction damage is often explained by factors such as whether ground improvement had been carried out or not and differences in the dates of reclamation. In the current study, elasto-plastic seismic response analysis of multi-layered ground was carried out using the results of ground surveys in Urayasu City and focusing attention on the existence of clay deposits deep in the liquefied ground and on their slanted geometry. The analysis showed that the existence of clay layer deposits at locations deeper than the liquefied layers caused amplification of the seismic wave in the somewhat long-period ranges, leading to large plastic strains sufficient to cause liquefaction even in intermediate soils that are usually considered to be resistant to liquefaction. In addition, it was shown that because of the existence of the sloped boundaries in the deep part of the ground, localized shear deformation became prominent in the inclined strata and caused nonuniform liquefaction to occur in the ground.

RÉSUMÉ: De graves dommages de liquéfaction ont été causés par le séisme océanique Tohoku-Pacifique dans la ville de Urayasu. L'ampleur des dommages de liquéfaction est spatialement non-uniforme et ses variations sont très irrégulières. La variation des dommages est souvent expliquée comme due à la présence d'amélioration des couches ou à la différence d'âge des polders. Dans cet article nous avons effectué une analyse de la réponse sismique elasto plastique des systèmes multicouches sur la base des résultats de l'analyse du terrain de Urayasu, en nous concentrant sur la présence de dépôts d'argile sur les parties profondes des strates liquéfiées et sur l'inclinaison de celles-ci. Le résultat montre qu'il est possible d'observer une liquéfaction des sols intermédiaires difficilement liquéfiables, suite à une déformation plastique due à une amplification de l'onde sismique dans la gamme des périodes longues lors de la présence d'argile déposée sur les couches plus profondes que les couches liquéfiées. En outre, la présence d'une limite inclinée en profondeur a montré que la déformation locale de cisaillement dans la partie inclinée prédomine, et que la liquéfaction se produit dans le sol de manière non uniforme.

KEYWORDS: liquefaction, stratum organization, stratum slope

1 INTRODUCTION

The 2011 off the Pacific coast of Tohoku Earthquake caused liquefaction to occur in reclaimed lands in Urayasu City and in other wide areas of reclaimed land along Tokyo Bay. Such liquefaction damage observed in the Kanto Region exhibited the following characteristics.

1) Extensive liquefaction damage occurred even though these areas were far away from the epicenter and the seismic intensity was only about 5 (the maximum acceleration in these areas was between 100 to 200 gal according to K-net and other ground acceleration measurement records).

2) Grain size distributions of samples taken in the vicinity of the areas where liquefaction occurred showed the amount of fine fraction to be large, although it had been considered hitherto that grounds with large fine fraction content are not easily liquefied.

3) The level of liquefaction damage was nonuniform spatially, and the variation in the damage levels was large.

Site survey and aerial photography data were used to produce Fig. 1, which illustrates the areas in Urayasu City where liquefaction damage was observed and those where such damage was not observed. The figure also indicates dates of reclamation work. Although liquefaction damage occurred over wide areas in the city, most of the damage is concentrated in relatively new reclaimed lands in a region between the city center and the southwest part of the city. In contrast, almost no damage occurred in the older land in the northwest part of the city. Newspaper and TV reports have attributed the extensive damage that occurred to the long durations of the tremors, and the difference in damage levels in various parts of Urayasu City has often been explained by the presence/absence of past

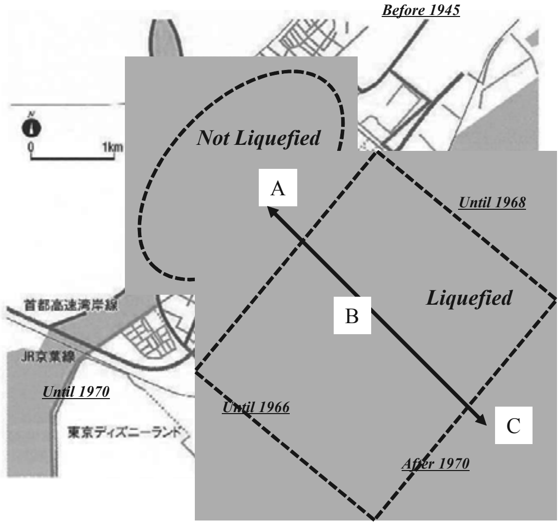

Figure 1. History of reclamation work in Urayasu City and distribution of liquefaction damage caused by the Great East Japan Earthquake (add and modified Nikkei Construction 2011)

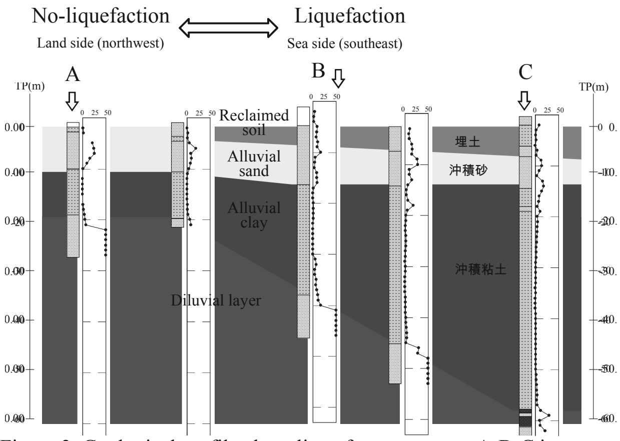

Figure 2. Geological profile along line of measurement A-B-C in Urayasu City

ground improvement and by the difference in the dates of reclamation work. Such causes of extensive damage are, no doubt, correct. However, sufficient explanations have not been provided yet concerning the mechanism of liquefaction occurrence in ground with large fine fraction content and the reason why the liquefaction damage was nonuniform.

Figure 2 shows the geological profile of Urayasu City along survey line A-B-C. Starting from the ground surface, the stratum organization broadly consists of reclaimed soil, alluvial sand, alluvial clay, and diluvial deposits, in that order. The reclaimed soil layer is nonhomogeneous, consisting of a complex mixture of sandy and clayey soils. The alluvial sand layer contains silty sand mainly made up of fine particles, the N-value being about 10 to 20. The alluvial clay layer is very weak with an N-value of approximately 0 to 1. Looking at the boundaries of the strata, it can be seen that the boundary between the alluvial sand and alluvial clay layers is almost horizontal, whereas that between the alluvial clay layer and the diluvial layer slopes downwards from Location A (land side, older reclaimed land) towards Location C (sea side, newly reclaimed land). Thus, the alluvial clay deposit is thicker towards Location C. The alluvial clay is about 10 m thick at Location A but extremely thick (more than 40 m) at Location C. Considering the liquefaction damage distribution shown in Fig. 1, it can be said that liquefaction damage was light at the land side locations, where the weak clay layer is relatively thin (about 10 m). Progressively heavier damage occurred towards the side of the sea along with the increase in thickness of the weak clay layer with an N-value of nearly zero.

This paper examines the cause of the extensive and nonuniform liquefaction damage that occurred in Urayasu City by focusing attention on the weak clay layer and its inclination in the deep part of the liquefied ground and carrying out elasto-plastic seismic response analysis of the multi-layer ground. The analysis code used was the soil-water coupled finite deformation analysis code GEOASIA (Noda et al. 2008), which incorporates an elasto-plastic constitutive model (SYS Cam-clay model; Asaoka et al. 2002) that allows description of the behavior of soils ranging from sand to intermediate soils and clay under the same theoretical framework.

2 DEPENDENCY OF SEISMIC BEHAVIOR OF GROUND ON THE ORGANIZATION OF DEEP STRATA

The effect of the weak clay layer in the deeper part of the ground on the reclaimed soil (silty sand containing fine fraction) was investigated using a one-dimensional model of locations A, B, and C in Fig. 2. Location B is midway between locations A and C. The finite element mesh used in the analysis and the

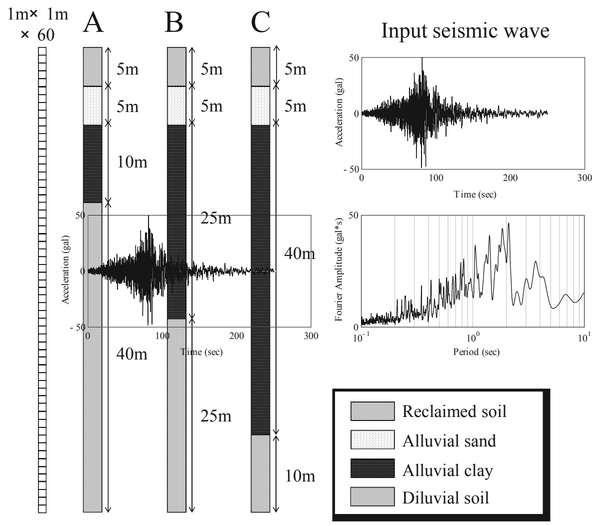

Figure 3. Finite element mesh and stratum organization at points A to C and input seismic wave

Table 1 Material constants and initial values used in the analysis

	Dilluvial deposit	Alluvial Clay	Alluvial Sand	Reclaimed Sand
Elasto-plastic parameters				
Critical state index M	1.00	1.60	1.00	1.70
NCL intercept N	2.10	2.50	2.00	2.50
Compression index $\tilde{\lambda}$	0.20	0.40	0.20	0.15
Swelling indes $\tilde{\kappa}$	0.0001	0.010	0.020	0.008
Poisson's ratio ν	0.10	0.10	0.35	0.10
Evolution parameters				
Degradation index of structure a	0.001	0.4	1.5	3.0
Ratio of $-D_v^p$ to $\|D_s^p\|$ c_s	1.0	0.3	0.3	0.1
Degradation index of OC m	50.0	20.0	0.7	2.0
Rotational hardening index br	0.0001	0.001	0.5	0.01
Limit of rotational hardening m_b	1.0	1.0	0.7	1.0
Initial conditions				
Specific volume v	1.70	3.30	2.30	2.90
Stress ratio η_0	0.545	0.545	0.545	0.545
Degree of structure $1/R^*_0$	10.0	20.0	15.0	10.0
Degree of anisotropy ζ_0	0.545	0.545	0.545	0.545
Soil particle density ρ_s (g/cm3)	2.65	2.65	2.65	2.65
Mass permeability index k (cm/s)	1.0×10^{-6}	5.0×10^{-7}	5.0×10^{-5}	1.0×10^{-5}

stratum organization at these three locations are shown in Fig. 3. The water pressure at the hydraulic boundary was made to be zero so as to make the ground coincide with the water level, and allowing for the existence of an impermeable layer with low hydraulic conductivity, the bottom face was assumed to be an undrained boundary. The two side faces, too, were assumed to be undrained boundaries. In addition, for defining the cyclic boundary (Noda et al. 2010) on the assumption that the same ground extends infinitely to the left and right sides, equal displacements were assigned as the constraint condition to each nodal element at the same height on both side faces. Table 1 shows the material constants and the initial values used in the analysis. Detailed soil surveys are still ongoing in Urayasu City. Therefore, the material constants used in this study were those of soils studied in the past at Nagoya University, which had physical properties relatively similar to the soils at the site. The reclaimed layer, which is assumed to be intermediate soil that is a mixture of sand and clay, is a material that is less prone to liquefaction than sandy soil. With respect to the initial values, it was assumed that the specific volume, degree of structure, stress ratio, and degree of anisotropy were uniform in the direction of depth. The overconsolidation ratio was distributed based on the overburden pressure. In locations A, B, and C, the conditions of

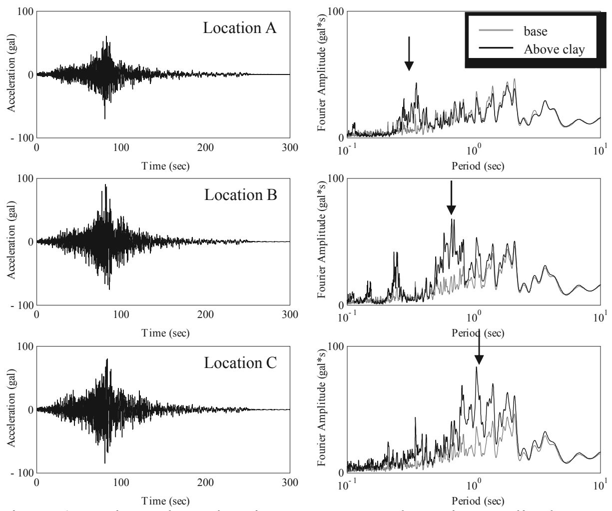

Figure 4. Horizontal acceleration responses and Fourier amplitude spectra after the seismic wave passed through the alluvial clay layers (alluvial clay/alluvial sand boundaries) at locations A, B, and C

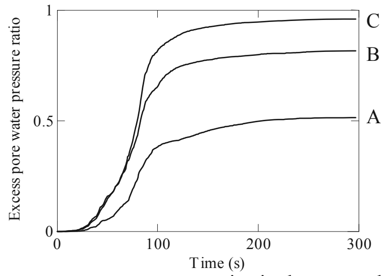

Figure 5. Excess pore water pressure ratios in the upper elements

the reclaimed layer and the alluvial sand layer are the same, and only the alluvial clay layer thickness (and diluvial deposit thickness) in the deep part of the ground is different. The input seismic waveform is also shown in Fig. 3. The seismic waveform observed in the deep part of the ground in Chiba Prefecture was obtained from Kik-net, amended on the basis of the Vs value, and input to the seismic bedrock in earthquake engineering at a depth of 60 m. The maximum acceleration is only several tens of gals. Equal accelerations were input in the horizontal direction to all nodal points, and based on on-site PS logging that is currently being carried out, viscous boundaries corresponding to Vs=300 m/sec were set in the horizontal direction at all these nodal points on the bottom face.

Figure 4 illustrates the horizontal acceleration responses and the Fourier amplitude spectra after the seismic wave passed through the alluvial clay layers (boundaries between alluvial clay and alluvial sand) at locations A, B, and C. Compared with the input seismic wave, there is almost no amplification of the acceleration at location A, where the clay layer is thin, but it can be observed that the acceleration is amplified as the thickness of the clay layer becomes larger. In addition, it can be observed from the Fourier amplitude spectra that the somewhat long-period components of the seismic wave in the vicinity of 0.5–0.7 sec at location B and 1–2 sec at location C have been amplified with increasing thickness of the clay layer. Figure 5 depicts the variation of excess pore water pressure ratio with time in the upper elements of the reclaimed layer. It is known through experience that a ground can be judged to have been liquefied if the excess pore water pressure ratio, which is an index obtained by dividing the excess pore water pressure by the effective overburden pressure before the earthquake, exceeds 0.95. In Fig. 5, the excess pore water pressures are seen to rise rapidly after 80 sec, which is in the vicinity of the time of maximum acceleration. In the case of location C, where the clay layer is thick, the excess pore water pressure ratio becomes nearly 1.0, indicating liquefaction. However, the stage of liquefaction has not been reached in the case of locations A and B. Development of large plastic strains is necessary for liquefaction to occur in intermediate soils with a fine fraction content. For the development of such large strains, large displacements and deformation caused by long-period ground motion together with several repeated loading cycles is required. As is clear from Fig. 4, the degree of amplification of acceleration becomes higher and the periodic band of amplified acceleration becomes larger with increasing thickness of the alluvial clay deposit in the deeper part of the ground. This is believed to be the reason why liquefaction occurred even in the case of silty sand with fine fraction content. This shows that, even if the conditions of the liquefied surface layers (reclaimed layer and alluvial sand layer) are the same, the level of liquefaction could vary solely due to the difference in the thickness of the alluvial clay deposits in the deeper part of the ground. Conventionally, in the FL method or simple microtopographic classification methods, only the "soil texture" of the surface layer becomes an issue, and other factors such as duration, stratum organization in deeper ground, etc. are not directly considered to be issues. The computed results described above suggest the necessity of utilizing leading-edge computational geomechanics based on elasto-plastic mechanics.

3 EFFECT OF THE INCLINATION OF DEEP STRATA ON THE SEISMIC BEHAVIOUR OF GROUND

In section 2 above, it was shown through one-dimensional elasto-plastic seismic response analysis of multi-layer ground at Urayasu City that the liquefaction damage observed in the ground with a fine fraction content was due to the presence of a thick layer of weak clay below the liquefied layer in addition to other factors such as the long duration of the earthquake and differences in the time of reclamation work execution. It was pointed out that in the weak clay layer, even if the maximum acceleration is small, there is a possibility of long-period acceleration responses occurring, leading to many repeated loading cycles that could cause development and storage of large strains and result in liquefaction. In this section, two-dimensional analysis was carried out taking account of the sloped boundary between the alluvial clay layer and the diluvial deposit below it. Figure 6 shows the finite element mesh used in the analysis. The width of the region analyzed is 6,000 m, and its depth is 60 m. In the 1800-m area at the middle of the region, a 2.2% slope was established at the boundary between the alluvial clay layer and the diluvial deposit, taking account of the actual stratum organization in Urayasu City (Fig. 2). The symbols A’, B’, and C’ in Fig. 6 indicate that these locations have the same stratum organizations as those of locations A, B, and C in the case of the one-dimensional model studied in section 2. Computational conditions such as ground conditions and boundary conditions were the same as in the analysis done in section 2.

Figure 7 illustrates the shear strain distribution 150 sec after earthquake occurrence. Only the area around the sloped part of the layer is shown in this figure, and the scale in the vertical direction has been magnified 8 times. Although shear strains are small in the non-inclined horizontal strata, large strains are produced in the reclaimed layer and in the sloped alluvial layer. Furthermore, this strain distribution is nonuniform and localized and increases with increasing thickness of the alluvial layer. The distribution of the excess pore water pressure ratio 150 sec after earthquake occurrence is illustrated in Fig. 8 and is seen to be nonuniform as in the case of shear strain. Liquefaction has occurred (excess pore water pressure ratios higher than 0.95) over a wide area in the sloped strata. Looking at the reclaimed layer, it can be seen that liquefaction has occurred at location

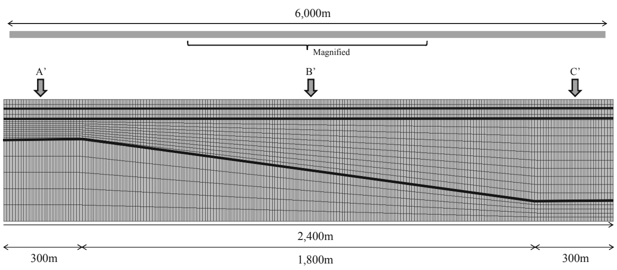

Figure 6. Finite element mesh used for the analysis

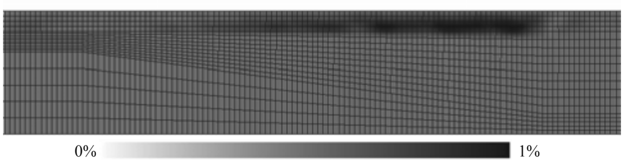

Figure 7. Shear strain distribution 150 seconds after the start of the earthquake

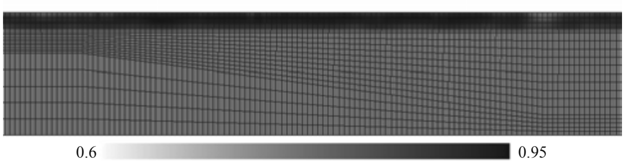

Figure 8 Excess pore water pressure distribution 150 seconds after the start of the earthquake

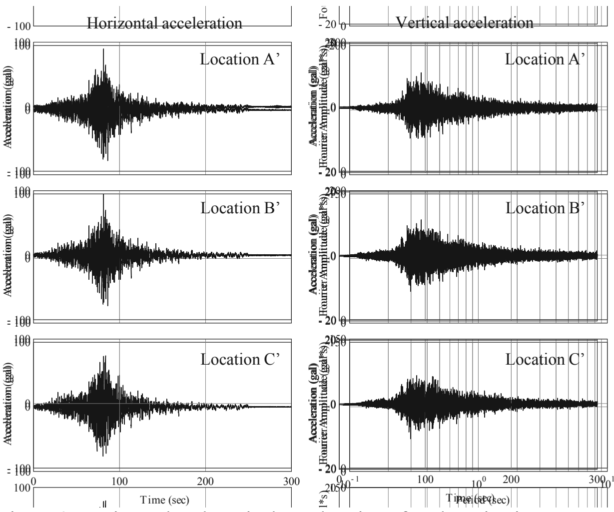

Figure 9. Horizontal and vertical acceleration after the seismic wave passed through the alluvial clay layers at locations A', B', and C'

B', which was not liquefied in the case of the one-dimensional model studied in section 2. The horizontal and vertical accelerations after the seismic wave passed through the alluvial clay layers (alluvial clay/alluvial sand boundaries) are shown in Fig. 9. There is not much difference in the horizontal accelerations when compared with those obtained through one-dimensional analysis. On the other hand, although there is almost no vertical acceleration response at location A', where the effect of the sloped stratum is small, vertical accelerations of up to about 10 gal have been generated at sloped locations B' and C'. The nonuniform, localized shear strain and excess pore water pressure ratio distributions illustrated in Figs. 7 and 8 are due to the input seismic wave being amplified in the clay layer (as explained in section 2) and the existence of the sloped boundary between the alluvial clay and diluvial layers, as shown through the analysis carried out in this section. In other words, in addition to the vertical component of seismic movement being generated by the stratum slope, multi-dimensional propagation is also exhibited because of complex reflection behavior in the diluvial layer. Moreover, in sloped layers such as location B', the danger of liquefaction is increased compared with the one-dimensional model. The actual liquefaction damage observed in Urayasu City was heavy in the sloped stratum locations where midterm reclamation work had been executed (mid-part of Fig. 1). This behavior resembles the results of the analysis carried out here. The current analysis shows that even in the case of homogeneous geomaterials, stratigraphic nonhomogeneity results in large variations in ground deformation behavior and that such deformation becomes particularly large in sloped strata locations. These things cannot be taken into consideration in one-dimensional analysis and highlight the necessity of performing multi-dimensional effective stress analysis.

4 CONCLUSIONS

Elasto-plastic seismic response analysis was carried out with respect to a multi-layered ground, focusing attention on the existence and slope of a clay layer deposited in the ground deeper than the liquefied layer. The results showed that the existence of the clay layer caused amplification of the seismic wave in the somewhat long-period ranges, leading to large plastic strains sufficient to cause liquefaction even in intermediate soils. In addition, it was shown that because of the existence of the sloped boundaries in the deep part of the ground, localized shear strains become prominent in the inclined strata and cause nonuniform liquefaction to occur in the ground. Although the materials/conditions of the ground studied here were not homogeneous, depending on the organization and slope of the strata, localized and nonuniform ground deformation could occur even in the case of homogeneous grounds. The factors mentioned above can be considered to have contributed to the heavy and nonuniform liquefaction damage observed in Urayasu.

5 ACKNOWLEDGEMENTS

The seismic wave input for the current study was obtained from the public database of the Strong-Motion Seismograph Network (KiK-net) of the National Research Institute for Earth Science and Disaster Prevention, and boring data obtained from the Chiba Prefecture Geological Environment Information Bank were used to assess the geological cross section of the ground. The authors wish to express their grateful thanks to these two institutions for providing the data. The authors would also like to extend their gratitude to the Ground Deformation Mechanism Research Committee of the Japanese Geotechnical Society for their kind cooperation in carrying out the current study.

6 REFERENCES

Nikkei Construction 2011. Lessons learnt from the Great East Japan Earthquake (The complete story of damage to infrastructures), 102-116. (in Japanese)

Asaoka et al. 2002. An elasto-plastic description of two distinct volume change mechanisms of soils. S&F, 42 (5), 47-57.

Noda et al. 2008. Soil-water coupled finite deformation analysis based on a rate-type equation of motion incorporating the SYS cam-clay model. S&F, 48 (6), 771-790.

Noda, T. et al. 2010. Modeling and Seismic Response Analysis of a Reclaimed Artificial Ground. ASCE Spec. Pub., No. 201, 294-299.

Noda, T. et al. 2009. Co-seismic and post-seismic behavior of an alternately layered sand-clay ground and embankment system accompanied by soil disturbance. S&F, 49 (5), 739-756.

Lysmer, J. and R.L. Kuhlemeyer 1969. Finite dynamic model for infinite media. ASCE, 95 (EM4), 59-877.

Asaoka et al. 2011. Effect of organization of deep strata on liquefaction of sandy surface layers with large fine fraction content. Program and Abstracts of the 2011 Fall Meeting of the Seismological Society of Japan, pp.56.